Schrödinger cat animated on a quantum computer

A. D. Chepelianskii[(a,b)], and D. L. Shepelyansky[(a)]
[(a)] *Laboratoire de Physique Quantique, UMR 5626 du CNRS, Université Paul Sabatier, 31062 Toulouse Cedex 4, France*
[(b)] *Lycée Pierre de Fermat, Parvis des Jacobins, 31068 Toulouse Cedex 7, France*
(Received: 2002.2002)

We present a quantum algorithm which allows to simulate chaos-assisted tunneling in deep semiclassical regime on existing quantum computers. This opens new possibilities for investigation of macroscopic quantum tunneling and realization of semiclassical Schrödinger cat oscillations. Our numerical studies determine the decoherence rate induced by noisy gates for these oscillations and propose a suitable parameter regime for their experimental implementation.

PACS numbers: 03.67.Lx, 05.45.Mt, 75.45.+j

Since 1935 until recently, the metaphor of Schrödinger cat oscillations between life and death [1] was considered as a purely theoretical concept. However, during the last decade such oscillations in a quantum limit were observed for two states of a Rydberg atom in a quantum cavity [2] and an experimental evidence was presented for a quantum superposition of macroscopically distinct states in a superconducting quantum interference device (SQUID) [3]. Manifestations of macroscopic quantum tunneling (MQT) were also observed in magnetization experiments with spin-ten molecular magnets Fe_8 and Mn_{12} [4,5]. In addition to their fundamental interest these experiments promise to provide important applications, e.g. for solid-state qubit realization [6] and information storage [7] based on the Grover algorithm [8].

The regime discussed in [1] assumes that the quantum tunneling takes place for a semiclassical object with a regular dynamics in two symmetric regions of phase space. Recently, the investigations of quantum chaos led to an extension of this concept to the phenomenon of chaos-assisted tunneling between islands of regular integrable dynamics separated by a chaotic sea [9]. In this case, due to chaos the period T_u of tunneling oscillations becomes very sensitive to the variation of system parameters and statistical description should be used to describe the average distribution of T_u [9–11]. This unusual tunneling is strongly influenced by complex instanton orbits and scarring effects [10,11] and a chaos enhancement of tunneling rate by orders of magnitude may be reached by a small variation of parameters. The first direct experimental observations of the chaos-assisted tunneling have been realized recently with cold [12] and ultracold atoms from a Bose-Einstein condensate [13] thus opening new possibilities for investigation of this interesting process. However, quantum tunneling is a very sensitive phenomenon and experimental studies are complicated by the decoherence produced by the environment. Due to that theoretical investigations of decoherence effects on MQT were initiated from the very beginning [14,15] and are continued up to now [16,17].

In this Letter, we show that quantum entanglement and quantum computer simulations [18] can be efficiently used to study quantum tunneling in deep semiclassical regime. We illustrate this on the example of a quantum symplectic map (double well map) which has a rich phase space structure with integrable islands surrounded by chaotic sea. Our algorithm has certain similarities with the algorithms for the kicked rotator [19] and for the sawtooth map [20]. It uses the quantum Fourier transform (QFT) [21] and simulates the dynamics of a quantum system with N levels in $O((\log_2 N)^4)$ operations per map iteration while any known classical algorithm requires at least $O(N \log_2 N)$ operations. Only one work space qubit is required for computations so that n_q qubits describe a physical system with $N = 2^{n_q-1}$ levels. Contrary to [20] the present algorithm simulates the quantum dynamics with mixed (chaotic/integrable) classical phase space and is optimal for the investigation of chaos-assisted tunneling in semiclassical regime. Indeed, while for MQT in molecular magnets [4,5,22] the effective Planck constant $\hbar$ is inversely proportional to the number of spins ($\hbar \propto 1/n_q$) in our algorithm $\hbar \propto 2^{-n_q}$. Hence with only 10 qubits the algorithm allows to study MQT with the semiclassical parameter being larger by almost two orders of magnitude. At present the nuclear magnetic resonance (NMR) quantum computer can perform QFT [23] and operate with up to 7 qubits [24]. This allows to study the chaos-assisted quantum tunneling on existing NMR based quantum computers and to obtain important information about decoherence effects in MQT regime.

In the classical limit the dynamics of our model is described by the double well map given by

$$\overline{p} = p - K dV(x)/dx \ , \quad \overline{x} = x + \overline{p} \quad (mod\ 2\pi). \qquad (1)$$

Here (p, x) are momentum and coordinate conjugated variables ($-\pi < x \leq \pi$), the bars denote the variables after one map iteration and $V(x) = (x^2 - a^2)^2$. In the limit $K \to 0$ the map gives the one-dimensional integrable dynamics in the double well potential $V(x)$ with the frequency of small oscillations $\omega_0 = 2\sqrt{2K}$. However, for $K > 0$ the higher harmonics of finite step iterations lead to appearance of chaotic component surrounding the stability islands located at $x = \pm a$. A typical example of mixed phase space is shown in Fig.1

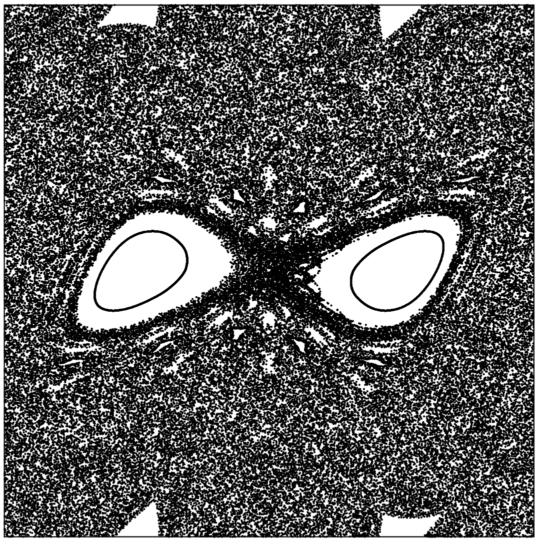

FIG. 1. Poincaré section for the double well map (1) at $K = 0.04, a = 1.6$, one chaotic and two regular orbits are shown in the cell $(-\pi \le x, p \le \pi)$.

The quantum evolution on one map iteration is described by a unitary operator $\hat{U}$ acting on the wave function ψ:

$$\overline{\psi} = \hat{U}\psi = e^{-i\hat{p}^2/2\hbar} e^{-iKV(x)/\hbar}\psi, \qquad (2)$$

where $\hat{p} = -i\hbar\partial/\partial x$ and $\psi(x+2\pi) = \psi(x)$. In the following we take the dimensionless $\hbar = 4\pi/N$ that corresponds to the case of quantum resonance [25] with two classical cells (e.g. as in Fig. 1) on a quantum torus containing N levels. The semiclassical regime corresponds to $\hbar \ll 1$ with discretized momentum $p = \hbar n$ where n is an integer. The most efficient known classical algorithm simulating the quantum dynamics (2) is based on forward/backward fast Fourier transform (FFT) between p and x representations. For a system with N levels it requires two FFT and two diagonal multiplications in p and x representations and can be performed in $O(N \log_2(N))$ operations.

The quantum algorithm simulates one map iteration (2) with $N = 2^{(n_q-1)}$ levels in $O(n_q^4)$ quantum gates operating on n_q qubits with one qubit used as a work space. The initial wave function in x representation is coded in the physical register with $n_q - 1$ qubits in equidistant discrete points x_m $|\psi(x)\rangle = \sum_{m=0}^{N-1} a_m |m\rangle|0\rangle$ with an empty work n_q−th qubit. The action of kick $U_k = \exp(-iKV(x)/\hbar)$ is diagonal in this representation and the simultaneous multiplication of all N coefficients can be done in $3n_q^4$ gate operations. Indeed, if $x = \sum_{j=0}^{n_q-2} \alpha_j 2^j$, then $x^4 = \sum_{j_1,j_2,j_3,j_4} \alpha_{j_1}\alpha_{j_2}\alpha_{j_3}\alpha_{j_4} 2^{j_1+j_2+j_3+j_4}$ and $e^{-i\beta x^4} = \Pi_{j_1,j_2,j_3,j_4} \exp(-i\beta\alpha_{j_1}\alpha_{j_2}\alpha_{j_3}\alpha_{j_4} 2^{j_1+j_2+j_3+j_4})$ with $\alpha_{j_{1,2,3,4}} = 0$ or 1. This step can be performed with approximately n_q^4 4-qubit gates, namely control-control-control–phase shift $(C^{(3)}(\beta))$. The gate $C^{(3)}(\beta)$ is applied to each group of 4 qubits and transfers $|1111\rangle$ to $\exp(-i\beta 2^{j_1+j_2+j_3+j_4})|1111\rangle$ keeping other combinations unchanged. Using the work qubit the gate $C^{(3)}(\beta)$ can be expressed via two Toffoli gates T and one control-control–phase shift $C^{(2)}(\beta)$ as $C^{(3)}_{j_1,j_2,j_3,j_4}(\beta) = T_{j_1,j_2,w} C^{(2)}_{w,j_3,j_4}(\beta) T_{j_1,j_2,w}$. Here the indices indicate the qubits on which the gates do apply, β notes the rotation angle and w is the work qubit, which is reset to 0 after $C^{(2)}(\beta)$. Thus, the action of kick is expressed via a sequence of standard gates used for quantum computations [21,26]. Indeed the Toffoli and $C^{(2)}(\beta)$ gates can be expressed via one and two qubit gates without addition of extra qubits [27]. The above computation is the most difficult step in the algorithm and takes approximately $2n_q^4$ Toffoli gates and n_q^4 of $C(\beta)$ gates for large n_q. The multiplications by kick phases with lower powers of x are done in the similar way and require smaller number of gates. After multiplication by U_k the algorithm is similar to the one used in [19,20]: the QFT changes

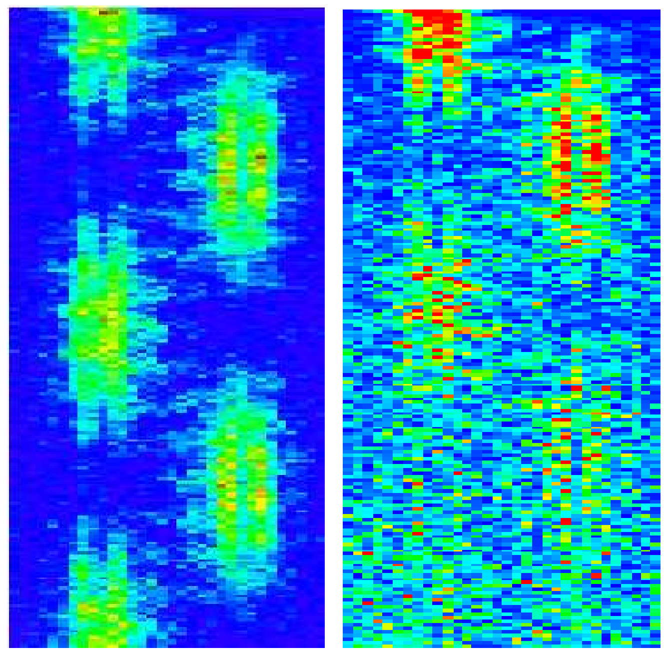

FIG. 2. (color) Time evolution of the Schrödinger cat: probability distribution $W(x)$ at $-\pi \le x \le \pi$ is shown for different number of map iterations t, changing along y-axis from $t = 0$ (top) to $t = 180$ (bottom). Here as in Fig.1 $K = 0.04, a = 1.6$ and $\hbar = 4\pi/N$ with $N = 2^{(n_q-1)}$. Quantum computation is done with $n_q = 6$ qubits, ideal perfect gates (left) and noisy gates of strength $\epsilon = 0.02$ (right), and $n_g = 2090$ gates per one map iteration (2). At $t = 0$ initial coherent packet is located at $x = -a$. The color is proportional to the density: blue for zero and red for maximal density.

x to p representation in $O(n_q^2)$ operations, the rotation $U_\hbar = \exp(-i\hbar n^2/2)$ is realized in n_q^2 of control–phase shift gates $C(\beta)$ and the backward QFT converts the wave function back to initial x representation.

An example of the Schrödinger cat oscillations simulated by this quantum algorithm with ideal gates in the regime of chaos-assisted tunneling of Fig.1 is shown in Fig.2 (left). The time evolution of the probability distribution $W(x)$, integrated over the work qubit, shows clear tunneling transitions between stability islands of Fig.1. The same evolution simulated by noisy gates is illustrated in Fig.2 (right). Noisy gates are modeled by unitary rotations by an angle randomly fluctuating in the interval $(-\epsilon/2, \epsilon/2)$ around ideal rotation angle. This noise introduces an effective decoherence rate Γ which destroys the tunneling oscillations after the time scale $1/\Gamma$.

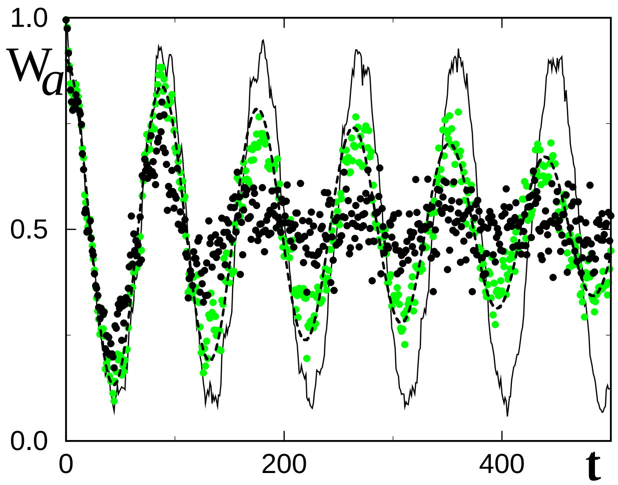

FIG. 3. Probability for the Schrödinger cat to be alive W_a (total probability for $x < 0$) as a function of time t for parameters of Fig. 2. The time dependence allows to determine the period of chaos assisted tunneling oscillations $T_u = 90$ and their decoherence decay rate Γ. Full curve shows the data without decoherece, points show the data for noisy gates with $\epsilon = 0.01$ (green) and $\epsilon = 0.02$ (black). The fit of data gives $\Gamma = 1.9 \times 10^{-3}$ (dashed curve for $\epsilon = 0.01$).

To determine the period of tunneling oscillations T_u and their decay rate Γ it is convenient to analyze the time dependence of total probability $W_a(t)$ at $x < 0$ (see Fig.3). The fit $W_a(t) - 1/2 \propto e^{-\Gamma t} \cos(2\pi t/T_u)$ allows to obtain both T_u and Γ. We note that the value of W_a at given t can be obtained efficiently from few measurements that enables to determine T_u and Γ. Moreover, the values of T_u and Γ are not sensitive to the choice of initial state at $t = 0$. As it was discussed in [28] for a similar situation, this state should only have a sufficiently large overlap with the coherent state in the center of stability island. For example, the step distribution, $W(x) = 2/N$ for $x < 0$ and $W(x) = 0$ for $x > 0$, which can be prepared efficiently, gives the same values of T_u and Γ as in the case of the coherent initial state.

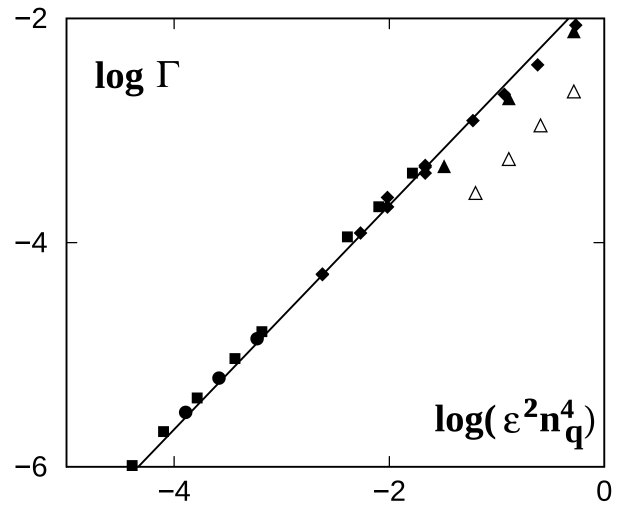

FIG. 4. Dependence of decoherence rate of tunneling oscillations Γ on the strength of gate noise ϵ for different number of qubits $n_q = 6$ (full triangles), 7 (diamonds), 8 (squares) and 9 (circles). The selected map parameters are varied in the range $1.4 \leq a \leq 1.7$, $0.04 \leq K < 0.06$ at $\hbar = \pi/2^{(n_q-3)}$ that gave the tunneling period variation in the range $90 \leq T_u \leq 1.8 \times 10^5$. The straight line shows the average dependence (3). The data with noiseless work qubit at $n_q = 6$ $(K = 0.04, a = 1.6)$ are shown by open triangles. Logarithms are decimal.

The dependence of the decoherence rate on the parameters is shown in Fig.4. The variation of Γ in a four orders of magnitude range is well described by the relation:

$$\Gamma = 0.021\epsilon^2 n_q^4 \tag{3}$$

This relation can be understood using the following physical arguments. For a given qubit, noise in each unitary gate gives a drop of the probability to be directed along the ideal direction by an amount of ϵ^2. Since at each map iteration the number of gates is $n_g \sim n_q^4$ the total decay rate is proportional to $\epsilon^2 n_g$ in agreement with Eq.(3). We note that similar estimates for the decoherence rate induced by noisy gates were also obtained for the Shor algorithm [29]. At the same time the relation (3) is rather simple comparing to the decoherence rates discussed for MQT in SQUIDs [14–16] and molecular magnets [17]. One of the reasons for that is that the main step of the algorithm operates always with the same work qubit. If the unitary rotations of this qubit are noiseless then the decay rate Γ is significantly reduced (see Fig. 4). Hence, the quantum error correcting codes [18] applied only to the work qubit can significantly reduce the decoherence rate, with a relatively small increase of the work space.

Our algorithm allows to obtain interesting results about chaos-assisted tunneling even with a small number of qubits. For example, the data of Fig. 3 can be obtained experimentally on the basis of techniques applied in [23,24]. The main obstacle for experimental implementation of this algorithm is the decoherence. Indeed to observe the Schrödinger cat oscillations the decoherence time scale $1/\Gamma$ should be much larger than the oscillation period T_u. As it is usually the case for semiclassical tunneling, the later increases exponentially with the decrease of $\hbar$. This implies very rapid growth of T_u with n_q: $T_u \propto \exp(S/\hbar) \propto \exp(2^{n_q} S/8\pi)$, where $S \sim 1$ is a constant related to the classical action. For example, for $K = 0.04,\ a = 1.6$ the period changes from $T_u = 90$ ($n_q = 6$) to $T_u = 1.68 \times 10^6$ ($n_q = 9$). Therefore even if the algorithm performs each map iteration (2) in polynomial number of gates, exponential number of map iterations should be done to observe tunneling oscillations in deep semiclassical regime. Nevertheless, in the regime of chaos-assisted tunneling, the value of S can be easily varied [9–11] by changing the parameters of the map (K and a) that allows to obtain not too large T_u values for $n_q \leq 10$, e.g. $T_u = 305$ for $K = 0.3, a = 0.5, n_q = 10$. Indeed, the value of S can be changed significantly by reducing the size of the stability islands embedded in the chaotic sea. In spite of the rapid growth of T_u with the number of qubits n_q the proposed algorithm uses them in an optimal way in order to reach the minimal effective Plack constant which scales as $\hbar \propto 2^{-n_q}$. This situation is qualitatively different comparing to SQUIDs [3] where even for a macroscopic number of particles (analogous to n_q) the evolution is described by a Hamiltonian with two levels and effective $\hbar \sim 1$ [16]. It also differs from the experiments [12,13] where effectively $\hbar \sim 1$ independently of number of cold atoms.

In summary, our studies show that the Schrödinger cat can be animated in a deep semiclassical regime on existing quantum computers [23,24] with six or more qubits. Such experiments will give interesting information about the nontrivial regime of chaos-assisted tunneling in presence of external decoherence. They will allow to determine the effective accuracy of quantum computation, operability bounds and decoherence rates for the first generation of quantum computers.

This work was supported in part by the NSA and ARDA under ARO contract No. DAAD19-01-1-0553, the NSF under Grant No. PHY99-07949 and the EC RTN contract HPRN-CT-2000-0156.

---

[1] E. Schrödinger, Naturwissenschaften **32**, 807 (1935).
[2] J.M. Raimond, M. Brune, and S. Haroche, Rev. Mod. Phys. **73**, 565 (2001).
[3] J.R. Friedman, V. Patel, W. Chen, S.K. Tolpygo, and J.E. Lukens, Nature **406**, 43 (2000).
[4] R. Sessoli, D. Gatteschi, A. Caneschi and A.M. Novak, Nature **365**, 141 (1993).
[5] J.R. Friedman, M.P. Sarachik, J. Tejada, and R. Ziolo, Phys. Rev. Lett. **76**, 3830 (1996).
[6] Y. Nakamura, Y.A. Pashkin and J.S. Tsai, Nature **398**, 786 (1999).
[7] M.N. Leuenberger and D. Loss, Nature **410**, 789 (2001).
[8] L.K. Grover, Phys. Rev. Lett. **79**, 325 (1997).
[9] O. Bohigas, S. Tomsovic, and D. Ullmo, Phys. Rep. **223**, 43 (1993).
[10] S.C. Creagh, and N.D. Whelan, Phys. Rev. Lett. **84**, 4084 (2000).
[11] W.E. Bies, L. Kaplan, and E.J. Heller, Phys. Rev. E **64**, 016204 (2001).
[12] D.A. Steck, W.H. Oskay, and M.G. Raizen, Science **293**, 274 (2001).
[13] W.K. Hensinger, H. Häffner, A. Browaeys, N.R. Heckenberg, K. Helmerson, C. McKenzie, G.J. Milburn, W.D. Phillips, S.L. Rolston, H. Rubinsztein-Dunlop, and B. Upcroft, Nature **412**, 52 (2001).
[14] A.O. Caldeira, and A.J. Leggett, Phys. Rev. Lett. **46**, 211 (1981).
[15] A.J. Leggett, S. Chakravarty, A.T. Dorsey, M.P.A. Fisher, A. Garg, and W. Zwerger, Rev. Mod. Phys. **59**, 1 (1987).
[16] Y. Makhlin, G. Schön, and A. Shnirman, Rev. Mod. Phys. **73**, 357 (2001).
[17] E.M. Chudnovsky and X. Martines-Hidalgo, cond-mat/0201184.
[18] For a review see, e.g., A.Steane, Rep. Prog. Phys. **61**, 117 (1998).
[19] B. Georgeot and D.L. Shepelyansky, Phys. Rev. Lett. **86**, 2890 (2001).
[20] G. Benenti, G. Casati, S. Montangero, and D.L. Shepelyansky, Phys. Rev. Lett. **87**, 227901 (2001)
[21] See, e.g., A. Ekert and R. Jozsa, Rev. Mod. Phys. **68**, 733 (1996).
[22] E.M. Chudnovsky and L. Gunther, Phys. Rev. Lett. **60**, 661 (1988).
[23] Y.S. Weinstein, M.A. Pravia, E.M. Fortunato, S. Lloyd, and D.G. Cory, Phys. Rev. Lett. **86**, 1889 (2001).
[24] L.M.K.Vandersypen, M. Steffen, G. Breyta, C.S. Yannoni, M.H. Sherwood, and I.L. Chuang, Nature **414**, 883 (2001).
[25] F. M. Izrailev, Phys. Rep. **196**, 299 (1990).
[26] V. Vedral, A. Barenco and A. Ekert, Phys. Rev. A **54**, 147 (1996);
[27] M.A. Nielsen, and I.L. Chuang, *Quantum Computation and Quantum Information*, Cambridge Univ. Press (2000) p.182.
[28] D.S. Abrams, and S. Lloyd, Phys. Rev. Lett. **83**, 5162 (1999).
[29] C. Miquel, J.P. Paz, and W.H. Zurek, Phys. Rev. Lett. **78**, 3971 (1997).